Mobile Traffic Forecasting for Maximizing 5G Network Slicing Resource Utilization

Vincenzo Sciancalepore*, Konstantinos Samdanis†, Xavier Costa-Perez*,
Dario Bega‡§, Marco Gramaglia‡§, Albert Banchs‡§
* NEC Europe Ltd. † Huawei Europe ‡ IMDEA Networks Institute § Universidad Carlos III de Madrid

***Abstract*—The emerging network slicing paradigm for 5G provides new business opportunities by enabling multi-tenancy support. At the same time, new technical challenges are introduced, as novel resource allocation algorithms are required to accommodate different business models. In particular, infrastructure providers need to implement radically new admission control policies to decide on network slices requests depending on their Service Level Agreements (SLA). When implementing such admission control policies, infrastructure providers may apply forecasting techniques in order to adjust the allocated slice resources so as to optimize the network utilization while meeting network slices' SLAs. This paper focuses on the design of three key network slicing building blocks responsible for (i) traffic analysis and prediction per network slice, (ii) admission control decisions for network slice requests, and (iii) adaptive correction of the forecasted load based on measured deviations. Our results show very substantial potential gains in terms of system utilization as well as a trade-off between conservative forecasting configurations versus more aggressive ones (higher gains, SLA risk).**

I. Introduction

In addition to the clear advantages in terms of, among others, enhanced bandwidth, reduced latency or extended coverage, the introduction of future 5G networks will have a significant impact on how operators manage their infrastructure. In contrast to the relatively monolithic architectures of 3G and 4G, by building on the recent advances in network *softwarization*, 5G networks will be highly modular and designed to be *future-proof*.

5G networks will hence allow higher flexibility: network virtualization can boost the introduction of very diverse services to be deployed on-demand using shared infrastructure. This feature enables new business opportunities for Mobile Network Operators (MNO); indeed, hosting different services with possibly conflicting requirements on the same infrastructure is currently not achievable with the current *one-size-fits-all* architectures. However, it also introduces new critical challenges; the network slicing concept [1] is expected to be one of the technical solutions to these challenges.

Network slicing allows MNOs to open their physical network infrastructure platform to the concurrent instantiation of multiple logical self-contained networks, orchestrated in different ways depending on their specific service requirements; such network slices are (temporarily) owned by the respective tenants. The availability of this vertical market provides new monetization opportunities of the network infrastructure, since (i) new players may come into play (e.g., automotive industry, e-health,...), and (ii) a higher infrastructure capacity utilization can be achieved by admitting network slice requests and exploiting multiplexing gains. In the above context, the technical enablers for network slicing admission control need to be investigated.

The 5G Network Slice Broker [2] is a novel network element that builds on the capacity broker functional block considered by 3GPP for advanced RAN sharing [3]. It maps incoming Service Level Agreement (SLA) requirements associated to network slice requests into physical resources. Tenants hence obtain a "slice" of the appropriate Radio Access Network (RAN) elements. The architectural specifications for this new network paradigm are currently under definition and the necessary algorithms yet to be devised.

Although very conservative mappings may be considered for mission critical services that need ultra-high availability, enhanced admission control algorithms that leverage multiplexing gains of traffic among slices are the key to the optimization of network utilization and monetization. To this end, the ability to predict the actual *footprint* of a particular network slice is essential to increase the maximum number of slices that might be run on the same infrastructure.

Building on this idea, in this paper we design three key network slicing building blocks: (i) a *forecasting* module that predicts network slices' traffic based on past traffic and user mobility, (ii) a network slicing *admission control* algorithm and (iii) a network slicing *scheduler* algorithm in charge of meeting the agreed SLAs and report deviations to the forecasting module.

The remaining of the paper is organized as follows. In Section II we review the state-of-the-art solutions, before presenting our framework building blocks in Section III. In Section IV we establish the basis of our slice forecasting model, whereas in Section V we formulate the admission control problem as a geometric knapsack, providing that this problem is NP-Hard. In Section VI we explain the slice scheduling process and how its feedback is used to adjust the forecasting process. In Section VII we discuss the simulation results and, finally, we conclude the paper in Section VIII.

II. Related Work

The support for multi-tenancy in 3GPP LTE networks is related to early proposals on active RAN sharing, which enables network sharing based on contractual agreements. A study on virtualization for wireless and mobile networks considering preliminary proposals such as the GENI project as well as early LTE base station virtualization is elaborated in [4]. Two active network sharing architectures are specified

This work has been partially funded by the European Union's Horizon 2020 research and innovation programme under the grant agreement No. 671584 5GNORMA.

in 3GPP, the Multi-Operator Core Network (MOCN), allowing each operator to share eNBs connected on a separate core network, and the Gateway Core Network (GWCN), where operators share additionally the Mobility Management Entity (MME) [5]. A complementary network sharing management, which enables MVNOs to control the allocated resources, is designed in [6]. Our proposal exploits the experience of early deployments, while being compatible with the 3GPP specifications.

A RAN sharing solution applying proportional fairness criterion is proposed in [7]. To share resources among different operators under diverse radio conditions, [8] introduces the Network Virtualization Substrate (NVS), a two-step process where the infrastructure first allocates resources to the virtual instances of eNBs and then each tenant customizes scheduling within its eNB instance [9]. In our work we adopt a similar two-step process, allocating slices via a broker entity that performs admission control based on the requested SLAs.

Our approach builds on the concept of a signaling-based network slicing broker solution by implementing a capacity forecasting algorithm that considers guaranteed and best-effort traffic in addition to user mobility. A study that explores different options of network sharing based on a centralized broker is provided in [10], considering mobility means, spectrum transfer policies and resource virtualization to optimize the usage of MNO's limited resources. Unlike our proposal, such a study introduces new 3GPP interfaces to accommodate the broker functionality. A scheme that integrates the capacity broker with a minimum set of enhancements on the 3GPP architecture is documented in [11]. Such capacity broker forecasts the network capacity when allocating guaranteed and best-effort slices, considering their respective SLAs. Our approach enhances previous solutions by introducing algorithms that dynamically evaluate network slices SLA requests, while maximizing the infrastructure resources utilization.

III. System Design

This paper builds on the concept of a 5G network slice broker in the context of the 3GPP network sharing management architecture [6] for establishing network slices through signaling. The 5G network slice broker is introduced in the network management system of the infrastructure provider to exploit 3GPP conventional monitoring procedures for gathering global network load measurements. Such information can assist the forecasting process, facilitating admission control while considering the specified network slice SLAs. To support a signaling-based slice allocation, certain 3GPP interfaces need to be enhanced (Type 5 and Itf-N) to enable the instantiation and configuration of network slices, indicating the time duration, the required resource amount, and additional requirements, such as, e.g., the slice SLA. We refer the reader to [2] for further architectural details.

Fig. 1 depicts the 5G Network Slice Broker building blocks addressed in this paper. Network slice requests are collected within a fixed negotiation time window. When the time window is closed, network slice requests are processed and evaluated. A key aspect for an efficient network slice admission control mechanism is to accurately predict the tenants' traffic evolution in the near future. This is achieved through a *Slice Forecasting* module in charge of analyzing the network slices traffic patterns and providing forecasting information to the *Admission Control* module, as explained in Section IV. When no forecasting solution is applied (w/o forecasting) or during the *training period* (for adjusting the forecasting algorithm parameters), the only information used are the SLA requests. Based on this information, Admission Control policies are applied in order to select which network slice requests will be granted for the next time window. To this end, two different algorithms are devised, with different performance and complexity features, as explained in Section V. The list of granted slice requests is sent to the *Slice Scheduling* module, which allocates network slice physical resources and monitors (with a penalty history function) the served traffic levels and potential SLA violations. Such a function is used to provide feedback to the forecasting module and thus adaptively adjust the system, as explained in Section VI.

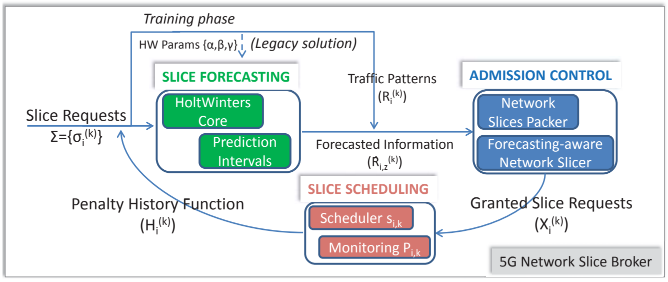

Fig. 1: Block diagram of the 5G Network Slice Broker.

IV. Slice Forecasting

Information on forecasted traffic patterns is used to predict future slice load and thus maximize the system resource utilization. The effectiveness highly depends on the accuracy of the forecasting algorithm: the more accurate, the more aggressive we can be in leasing available resources while keeping a small probability of violating slice SLAs. While the first aspect is deeply analyzed in this section, we refer the reader to Section VI for more details on SLA violations and dynamic forecasting parameters adjustments.

A. Tenant traffic analysis: characterization and forecasting

Traffic predictions are performed on an aggregate basis for every tenant. Each tenant i might ask for a different network slice request tailored to its specific service requirements. Indeed, the forecasting process can easily categorize the traffic requests based on the associated service requirements, thereby performing a prediction separately per slice. In our analysis, we first assume that traffic requests are uniformly distributed within the whole network. However, in Section IV-B we extend this assumption by considering multi-cellular environments where tenant traffic requests are significantly affected by the user mobility.

We assume different classes of traffic based on specific SLAs, as shown in Table I. We let the traffic volumes of tenant i for traffic class k (e.g., satisfying particular service requirements) be a realization of a point process, $\zeta_i^{(k)} = \sum_{t=0}^{T} \delta_t \, r_i^{(k)}(t)$, where δ_t denotes the Dirac measure for sample t. We express traffic requests $r_i^{(k)}(t)$ in terms of required resources (note that these resources could be easily translated into different metrics, such as latency or throughput demands). Given the periodic nature of traffic requests, the traffic forecasting is based on an observed time window T_{OBS}, and is given by the vector $\mathbf{r_i^{(k)}} = (r_i^{(k)}(t - T_{\text{OBS}}), r_i^{(k)}(t - (T_{\text{OBS}} + 1)), \cdots, r_i^{(k)}(t))$. Then, the forecasting function f_{HW} provides forecasted traffic volumes for time period $[t+1, t+T_{\text{WINDOW}}]$, denoted as $\hat{\mathbf{r}}_{\mathbf{i}}^{\mathbf{(k)}} = (\hat{r}_i^{(k)}(t+1), \hat{r}_i^{(k)}(t+2), \cdots, \hat{r}_i^{(k)}(t+T_{\text{WINDOW}}))$. For fixed traffic patterns, the system exhibits a periodic behavior, which translates into seasons of length W_S that are repeated over time. Within a single season we assume that process $\zeta_i^{(k)}$ is stationary and ergodic. Thus, we can use the Holt-Winters (HW) forecasting procedure to analyze and predict future traffic requests associated to a particular network slice. We denote a specific predicted traffic request $\hat{r}_i^{(k)}(t)$ by $\hat{r}_{i,t}^{(k)}$. We rely on the additive version of the HW forecasting problem as the seasonal effect does not depend on the mean traffic level of the observed time window but instead it is added considering values predicted through level and trend effects. Following HW standard procedure, we can predict such requests based on the level l_t, trend b_t and seasonal s_t factors, as follows:

$$\begin{aligned}\hat{r}_{i,t+T_{\text{WINDOW}}}^{(k)} &= l_t + b_t h + s_{t+T_{\text{WINDOW}}-W} \quad \text{where}\\ l_t &= \alpha(r_{i,t}^{(k)} - s_{t-W}) + (1-\alpha)(l_{t-1} + b_{t-1}),\\ b_t &= \beta(L_t - l_{t-1}) + (1-\beta)b_{t-1},\\ s_t &= \gamma(r_{i,t}^{(k)} - l_{t-1} - b_{t-1}) + (1-\gamma)s_{t-W}.\end{aligned} \tag{1}$$

While the set of optimal HW parameters α, β and γ can be obtained during a training period employing existing techniques [12], we focus on the forecasting errors and how the forecasting inaccuracy may affect our network slicing solution. We define the one-step training forecasting error $e_{i,t}^{(k)}$ as follows

$$e_{i,t}^{(k)} = r_{i,t}^{(k)} - \hat{r}_{i,t}^{(k)} = r_{i,t}^{(k)} - (l_{t-1} + b_{t-1} + s_{t-1}), \tag{2}$$

which is computed during the training period of our forecasting algorithm (when predicted values are compared with the observed ones). Given that our process $\zeta_i^{(k)}$ is ergodic and assuming an optimal HW parameter set, for any predicted value at time z we can derive the prediction interval $\left[\hat{ll}_{i,z}^{(k,\chi)}, \hat{hh}_{i,z}^{(k,\chi)}\right]$ wherein future traffic requests lie for that particular network slice with a certain probability $\chi_i^{(k)}$. Then, it holds that

$$Pr\left\{\hat{ll}_{i,z}^{(k,\chi)} \leq \hat{r}_{i,z}^{(k)} \leq \hat{hh}_{i,z}^{(k,\chi)}\right\} = \chi_i^{(k)}, \forall z \in [t+1, t+T_{\text{WINDOW}}] \tag{3}$$

where $\hat{hh}_{i,z}^{(k,\chi)}(\text{or } \hat{ll}_{i,z}^{(k,\chi)}) = \hat{r}_{i,z}^{(k)} + (-)\Omega_\chi\sqrt{Var(e_{i,z}^{(k)})}$ and

$$Var(e_{i,z}^{(k)}) \approx \left((1 + (z-1)\alpha^2[1 + z\beta + \frac{z(2z-1)}{6}\beta^2]\right)\sigma_e^2.$$

In the above equation, Ω_χ denotes the one-tailed value of a standard normal distribution such that we obtain $\chi_i^{(k)}$ probability and σ_e^2 is the variance of one-step training forecasting error, i.e., $\sigma_e^2 = Var(e_{i,t}^{(k)})$, over the observed time window.

TABLE I: Network slice traffic requirements [13]

k	$T^{(k)}$	Type and QCI
0	10 ms	GBR - 65
1	50 ms	GBR - 3
2	100 ms	GBR - 1
3	150 ms	GBR - 2
4	300 ms	non-GBR - 6
5	1000 ms	non-GBR - 9

Due to the penalties imposed by traffic SLAs, we focus only on the upper bound of the prediction interval as it provides the "worst-case" of a forecasted traffic level. From Eq. (3), a larger prediction time window T_{WINDOW}, e.g., a higher number of predicted values z, leads to a lower accuracy and behaves closer to the real network slice demand (limited network slice resources utilization). Conversely, an accurate forecasting with a lower error probability can result in severe penalties in case it does not guarantee the desired slice SLAs. Therefore, we adjust the forecasting error probability $\chi_i^{(k)}$ according to the service requirements and to the number of prediction points the forecasting process needs to perform. For instance, best-effort traffic requests having no stringent requirements can tolerate a prediction with a longer time pace that results in imprecise values. This makes the upper bound $\hat{hh}_{i,z}^{(k,\chi)}$ very close to the real (future) values $r_{i,z}^{(k,\chi)}$ regardless the error probability $\chi_i^{(k)}$ as the number of z values to predict is limited. Hence, we might select a low forecasting error probability $\chi_i^{(k)}$ for this service type. On the other hand, when guaranteed bit rate traffic is considered, the corresponding SLA must be fulfilled in a shorter time basis, which makes our forecasting process much more complex, requiring significantly more predicted values z. To achieve this, our system models such a type of traffic with a higher forecasting error probability $\chi_i^{(k)}$.

We implement the above mathematically as follows. According to the traffic classes defined in Table I, traffic class $k = 0$ provides a forecasted horizon shorter than the other traffic classes, and hence a larger number of values z must be predicted. To achieve this, we can derive an upper bound for the forecasting probability error per tenant i for this traffic class. We calculate the maximum potential gain between the slice request and the forecasted traffic requests as $\hat{d}_i^{(k)} = \max\limits_{z \in \text{T}_{\text{WINDOW}}} \left(R_i^{(k)} - \hat{r}_{i,z}^{(k)}\right)$. We then compute the forecasting error probability as follows

$$\chi_i^{(k=0)} : \Omega_\chi\sqrt{Var(e_{i,z}^{(k=0)})} = \hat{d}_i^{(k=0)}. \tag{4}$$

As soon as the potential gain $\hat{d}_i^{(k=0)}$ becomes very large, we cap the one-tailed value Ω_χ to 3.49, resulting in $\chi_i^{(k=0)} = 99.9\%$. Conversely, for the best-effort traffic ($k = 5$) we compute the forecasting error probability $\chi_i^{(k=|\mathcal{K}|)} = 50\%$, due to its more relaxed service. For the other traffic classes k, intermediate forecasting error probabilities $\chi_i^{(k)}$ are calculated from (4) by deriving $\hat{d}_i^{(k)}$ values from the upper and the lower bound values. However, note that forecasting error probability values are dynamically evaluated and adjusted based on the SLA violations experienced during the slice scheduling process, as explained in detail in Section VI-B.

B. User mobility and traffic model periodicity

We next extend our forecasting model to dynamic scenarios where user mobility is considered and the traffic periodicity assumption no longer holds. We consider a multi-cellular environment covering the whole area. In order to design forecasting algorithms that are accurate under realistic settings, we rely on human-based mobility patterns. Specifically, we employ the well-accepted SLAW mobility model [14] for user motions. According to this model, users move among a number of waypoints, which are distributed over the network area according to self-similarity rules forming a given number of clusters. Clusters with more waypoints can be seen as hotspots attracting more users. While performing a flight (a movement from one waypoint to the other within the same trip), based on some given probabilities users choose a set of clusters which are dynamically and randomly replaced during the flight. Then, users start moving between a subset of waypoints residing within the selected clusters according to a least-action trip planning (LATP) with $\alpha_{\text{SLAW}} = 3$. Traffic requests come randomly during the user trip. Assuming that users stop when reaching a waypoint for a pause-time, we can model the value of the flight-time (x_L) and pause-time (x_P) as a random value drawn from a heavy-tailed distribution function defined in terms of Fourier transformations as

$$f_L(x) = f_P(x) = \frac{1}{2\pi} \int_{-\infty}^{\infty} e^{-iu\,x - |\rho u|^{\alpha_{\text{DISTR}}}} \mathrm{d}u \qquad (5)$$

where ρ is the scale factor and α^{DISTR} depends on the distribution considered (pause-time or flight-time).

Given a uniform user speed distribution, the traffic model of the considered users is dominated by a heavy-tailed distribution whose components can be decoupled, as showed in Eq. (5). Under these conditions, the system exhibits a periodic behaviour (like in the previous section). Without loss of generality, we can obtain a periodic traffic vector as follows. Let M denote the period and $\mathbf{r}_{\mathbf{i}}^{(\mathbf{k})} = \{r_t\}$ a generic traffic vector. Then, the forecasting process applies a Discrete Fourier Transform (DFT) to retrieve the M-periodic samples $R_w = \sum_{n=0}^{M-1} r_t e^{-iw\frac{2\pi}{N}t}$, where $w = 0, \cdots, M-1$. Note that R_w is a complex number translating the sinusoidal component of r_t. Then, the forecasting process can obtain all single time-series components derived by each of those frequency samples by applying the Inverse Discrete Fourier Transform (IDFT), e.g., $r_n = \frac{1}{N}\sum_{w=0}^{M-1} R_w e^{\frac{2\pi i}{Nwn}}$, where $n = 0, \cdots, N-1$, which provides a periodic traffic vector $\mathbf{r}_{\mathbf{i}}^{(\mathbf{k})} = (r_i^{(k)}(n), r_i^{(k)}(n+1), \cdots, r_i^{(k)}(n+M))$.

V. Admission control: Design and validation

A 5G Network Slice Broker might decide on the network slice requests to be granted for the subsequent time window T_{WINDOW} based solely on the current resource availability. However, if forecasting information is taken into account, the resources consumed by network slice requests might be accurately reshaped to fit additional slice requests into the system (see Fig. 2).

A mathematical approach is proposed next address the admission control problem for both cases. First, we prove its NP-Hardness and suggest a baseline algorithm for allocating network slice requests when no forecasting information is available. Then, we design the Forecasting-aware Network Slicer algorithm to efficiently perform the admission control phase exploiting accurate traffic pattern predictions.

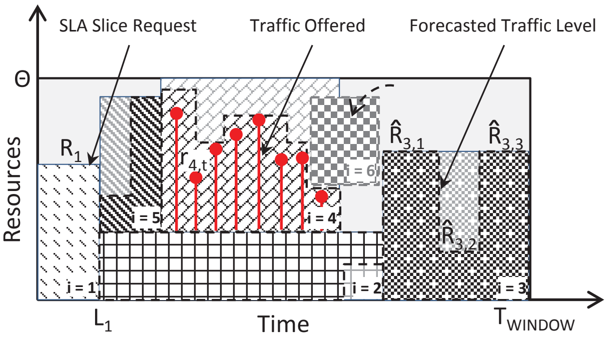

Fig. 2: Admission control problem as geometric knapsack problem.

A. Problem Formulation

In our problem formulation, we first assume that network slice instantiations require a constant amount of resources, and then we show that, when relaxing such an assumption by considering different forecasted traffic levels, the problem becomes more complex but still tractable for our admission control process.

Let us define a network slice request as $\sigma_i^{(k)} = \{R, L, i, k\}$ where i identifies the tenant, R is the amount of resources required, L is the time duration of the slice and k is the traffic class. Hereafter, we simply refer to a tenant request as $R_i^{(k)}(L_i)$. Recalling that our main objective is to accommodate network slice requests within a fixed time window T_{WINDOW} while maximizing the network resource utilization, we next derive our model.

Let us assume a rectangular box with fixed width W and height H representing the resource availability within a fixed time window. In particular, the box width corresponds to T_{WINDOW} and box height corresponds to the total amount of resources Θ. Let us assume a set of items $\mathcal{I}$, where each item $i \in \mathcal{I}$ corresponds to a network slice request having width w_i (corresponding to slice duration L_i) and height h_i (corresponding to the amount of resources R_i). In addition, each item provides a profit c_i that corresponds to the amount of resources needed (here we are assuming that a slice request pays an amount of money proportional to the number of resources granted[1]). Then, the objective of our admission control problem is to find a subset of items $\mathcal{I}' \subseteq \mathcal{I}$ that maximizes the total profit $\sum_{i \in \mathcal{I}'} c_i$, i.e., the total amount of used resources, as shown in Fig. 2.

Lemma 1. *Let the overall system resource availability be a box with height Θ and width T, and let each item $i \in \mathcal{I}$ be the network slice request σ_i with height R_i and width L_i. Then, the admission control problem is mapped into a Geometric Two-dimensional knapsack problem with the objective of filling*

[1] This assumption could be relaxed to reflect a different economic model within the multi-tenancy framework, which is out of the scope of the paper.

up our system capacity with network slice requests while maximizing the network resource utilization.

Let us now consider tenant requests that are characterized by a set $\hat{R}_{i,z}^{(k)} = \hat{hh}_{i,z}^{(k,\chi)}$ representing the predicted amount of needed resources at time z for a traffic type k (provided by the forecasting phase as a function of the forecasting error probability $\chi_i^{(k)}$). This results in time-variant resource requests with shapes that are no longer rectangular.

Lemma 1a. *Let the overall system capacity be a box with height Θ and width T, and let each item $i \in \mathcal{I}$ be the network slice request σ_i with irregular shapes, identified by different height values $R_{i,z}^{(k)}$ and width L_i. Then, the admission control problem is mapped into a Flexibile Geometric Two-dimensional knapsack problem, with the objective of maximizing the network resources utilization whilst accommodating network slice requests.*

An illustrative example is provided in Fig. 2, wherein different amounts of resource values are forecasted for a single network slice request. It may be observed that when the forecasting is accurate, i.e., the predicted values are close to the real traffic ones (as it is the case for slice $i = 4$, where real traffic is shown with the red points), there is more room to accommodate additional slices (such as slice $i = 6$ in the example). Please note that in our case the (flexible) geometric two-dimensional knapsack problem is constrained by the orientation law of the considered items. In particular, each item i has a fixed orientation, which can not be changed to fit in the box [2]. We can formulate our admission control problem as follows [3]

Problem ADM−CONTROL:

$$\begin{aligned} \text{maximize} \quad & \sum_{i \in \mathcal{I}} c_i \cdot x_i \\ \text{subject to} \quad & \sum_{i \in \mathcal{I}} w_i \cdot x_i \leq W; \qquad \text{(relaxed)} \\ & \mathcal{S}(x_i) \cap \mathcal{S}(x_k) = \emptyset, \quad \forall i \neq k; \\ & \mathcal{S}(x_i) \subset \mathbb{S}, \qquad \forall i \in \mathcal{I}; \\ & x_i \in [0,1], \qquad \forall i \in \mathcal{I}; \end{aligned}$$

where $\mathcal{S}(x_i)$ corresponds to the geometrical area of the item i (either rectangular or irregular) whereas $\mathbb{S}$ is the area of the box, i.e., $|\mathbb{S}| = T \cdot \Theta$. The given constraints impose that items cannot overlap with each other and must be contained within the total space of the box. The solution of this problem provides a set of x_i values, each of which is a binary value indicating whether the item i is admitted into the system or rejected for the next time window T_{WINDOW}, i.e., a list of granted slice requests in Fig. 1.

B. Complexity Analysis

We now analyze the complexity of the admission control problem, while in the next section we provide practical algorithms for this problem. In order to analyze the complexity, we formulate the following decision problem DEC−ADM−CONTROL: *given an arbitrary value V, n items with a value c_i and a given area a_i enclosed within a two-dimensional shape identified by $R_{i,z}^{(k)}$ and L_i, and a box with capacity $\mathbb{S}$ delimited by Θ and T, is there a subset $\mathcal{I} \in \{1, 2, \cdots, n\}$ such that items do not overlap and $\sum_{i \in \mathcal{I}} c_i \geq V$?*

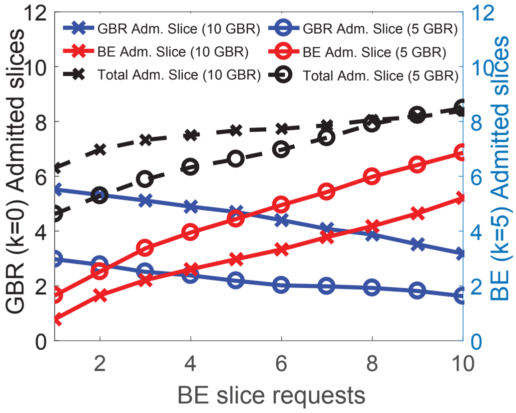

Fig. 3: Admitted slice requests within a time windows while collecting slice requests with GBR traffic requirements ($k = 0$) and best-effort traffic requirements ($k = 5$).

Lemma 2. *Considering all items with full flexible dimensions, we can identify one single weight w_i per item representing the area required. Then, if the utility value $c_i = w_i$ the decision problem DEC−ADM−CONTROL reduces to a "Subset Sum Problem".*

Theorem 1. *The decision problem DEC−ADM−CONTROL is NP-Complete and Problem ADM−CONTROL is NP-Hard for any type of traffic k along the network slice request.*

Sketch of Proof: We use a reduction from the subset sum problem based on Lemma 2. We apply a polynomial reduction to the decision problem DEC−ADM−CONTROL considering only items with full flexible dimensions collapsed into a weight w_i and utility value equal to the weights $c_i = w_i$. This reduces the problem to a Subset-Sum problem, known to be NP-COMPLETE. When considering items with fixed resource provisioning, i.e., items with constrained shape values, it is even more difficult to find a solution to Problem DEC−ADM−CONTROL, which proves the NP-Completeness. Based on this, we have that for all $\epsilon > 0$ approximating the solution for Problem ADM−CONTROL, $|\mathcal{I}| = n$ within $n^{1-\epsilon}$ is NP-Hard. This proves that our Problem ADM−CONTROL is NP-Hard. □

Theorem 1 suggests that no optimal polynomial time algorithm can solve our admission control problem. Interestingly, note that the admission control problem is easier when only best-effort slice requests are processed (although it is still NP-Hard). Moreover, with best-effort or less-demanding traffic, the number of request that can be admitted is higher, as confirmed by the results of Fig. 3. In this figure, we consider two different traffic classes, a traffic class with class requirements GBR ($k = 0$) and best-effort (BE) class ($k = 5$), and depict the

[2] Although some state-of-the-art work calls such a problem constrained geometrical knapsack problem, we prefer to omit the "constrained" word as it may refer to additional constraints on the relationship between items stored in the box, which are out of the scope of this work.

[3] In addition to the constraints included in our probelm formulation, the Flexibile Geometric Twodimensional knapsack problem also includes an additional constraint on weight capacities. For the sake of simplicity, we have omitted this constraint in our problem.

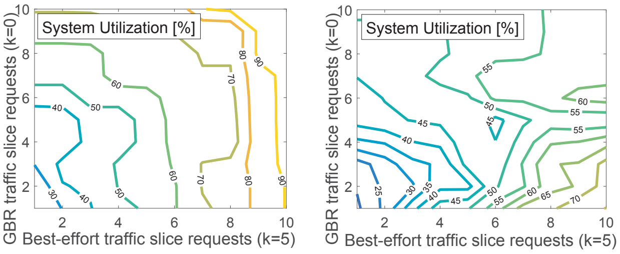

(a) $\eta = 0$; no inter-class priority (b) $\eta = 1$; inter-class priority

Fig. 4: System utilization with different utility functions.

number of admitted slice requests as a function of the demands of each class to the 5G Network Slice Broker. We observe that the total number of admitted slices increases with the number of best-effort slice requests, showing that best-effort slice requests are preferred due to the higher flexibility. This is further supported by Fig. 4(a), which shows the contour of the total system utilization when different number of slice requests are issued to the network. We observe that utilization is maximized when the number of BE slice requests is high, reaching values as high as 90% in the best case. The results provided above show a preferential treatment to the less demanding traffic classes, which may negatively affect the performance of the other classes. In order to overcome this problem, in the following we provide a smart mechanism which ensures no traffic inter-class prioritization. We define the utility value in Problem ADM−CONTROL for each slice requests as $c_i = \frac{L_i R_i}{(T^{(k)})^{\eta}}$, with $\eta \in \{0, 1\}$. For $\eta = 0$, the utility value for all classes is equal to the amount of data required within the slice, whereas with $\eta = 1$ we provide a higher priority to service classes with more strict requirements. In Fig. 4(b) we show the contour of the system utilization for $\eta = 1$. With this setting, we improve the inter-class fairness level (as shown in the top-right part of the picture), but this comes at the price of degrading the overall utilization (which does not exceed 55% in the best case).

C. Heuristic algorithm design

The admission control needs to optimize the total utility function while coping with different network slice requests, following the formulation in Problem ADM−CONTROL. We distinguish the following two types of network slice requests: (i) regularly shaped, when no forecasted information is considered, and (ii) irregularly shaped, depending on the predicted load at each point in time. For both request types, we may have different flexibility degrees depending on the traffic class considered. In the following, we propose algorithms for the two types of network slice requests. The first type is handled through a Network Slices Packer algorithm, a revised and improved version of [15]. The second type of network slice problem admits at least the same solution of the first class but, if properly explored, it could provide a higher resources utilization.

Network Slices Packer. We consider rectangular shapes for network slice requests with different traffic requirements. When traffic class $k = 0$, the regular shape of the network slice is strictly defined and no flexibility is allowed for allocating the traffic requests. Conversely, when less-demanding slice requests $k > 0$ are considered, the slice might be reshaped, delaying the slice traffic, to efficiently fit into the network.

Algorithm 1 Network Slices Packer: Algorithm to admit network slice requests $\sigma_i^{(k)}$ within the system capacity Θ for the next time window T_{WINDOW}.

```
 Input: $\Sigma = \{\sigma_i^{(k)}\}, \Theta, T_{\text{WINDOW}}, \mathbb{S}$
 Initialization: $\mathcal{C} \leftarrow \emptyset, \mathcal{F}_1 \leftarrow \emptyset, \mathcal{F}_2 \leftarrow \emptyset, \mathcal{E} \leftarrow \emptyset$
 Procedure
 1: for all $C_l \leftarrow \binom{\Sigma}{2}$ do
 2:     if $C_l$ fits into $\mathbb{S}$ then
 3:         $\mathcal{C} \leftarrow \mathcal{C} \cup C_l$
 4:     end if
 5: end for
 6: for all $C_l \in \mathcal{C}$ do
 7:     $\{v(C_l \cup B_l), s(C_l \cup B_l)\} \leftarrow$ Solve the knapsack problem $P(C_l)$
 8: end for
 9: $l* = \arg\max_{l \in \mathcal{C}} \{v(C_l \cup B_l)\}$
10: if $v(C_{l*}) \geq \frac{v(C_{l*} \cup B_{l*})}{2}$ then
11:     return $C_{l*}$
12: else
13:     $\mathcal{F}_1 \leftarrow C_{l*}$
14:     $\mathcal{F}_2 \leftarrow B_{l*}$
15:     if $s(\mathcal{F}_1) \geq \frac{|\mathbb{S}|}{2}$ then
16:         return $B_{l*}$
17:     else
18:         Sort $\mathcal{F}_2$ in non-increasing order of their profits and traffic class $k$
19:         while $s(\mathcal{F}_1) < \frac{\mathbb{S}}{2}$ do
20:             e = pop($\mathcal{F}_2$)
21:             $\mathcal{F}_1 \leftarrow \{\mathcal{F}_1 \cup e\}$
22:         end while
23:         if $v(\mathcal{F}_2) \geq \frac{v(C_{l*} \cup B_{l*})}{2}$ then
24:             return $v(\mathcal{F}_2)$
25:         else
26:             $\mathcal{E} \leftarrow \max\{v(\mathcal{F}_1 \setminus e); v(\mathcal{F}_2)\}$
27:             return $\mathcal{E}$
28:         end if
29:     end if
30: end if
```

We make the assumption that each tenant is not allowed to ask more than the half of the resource availability of the infrastructure provider, i.e., $R_i \leq \frac{\Theta}{2}$. This implies that at least 2 network slices can be possibly accommodated. The algorithm pseudocode is given in Algorithm 1. Among all possible pairs of network slice requests, only those fitting the available system capacity are taken into account (line 2). For each 2-slice set (C_l), we formulate a 0-1 knapsack problem to maximize the total profit considering that the profit of each item is given by the area of the slice $(R_i \cdot L_i)$. The item set to evaluate for the knapsack problem includes the 2-slice set (C_l) and all the other slices (B_l). Following the FPTAS proposed in [16], we retrieve the best solution, i.e., a set of network slice requests $(C_{l*} \cup B_{l*})$ among all knapsack problems (line 9). If the total profit $v(\cdot)$ assigned to the 2-slice set requests C_{l*} is greater than the half of the best profit retrieved after running all knapsack problems, we keep C_{l*} as the best feasible set (line 10-11). Otherwise, we split the optimal set into two subsets $\mathcal{F}_1$ and $\mathcal{F}_2$ (line 13-14). If the total space covered by the items in $\mathcal{F}_1$ is greater than the half of the total system capacity area (line 15), this implies that the second subset $\mathcal{F}_2$ will cover less then the half of the available system capacity[4], and provide a total profit greater than the half of the optimal solution. In

[4] Based on the Steinberg's theorem, if the sum of the item areas are less than the half of the box, they can be packed. See A. Steinberg, "A strip-packing algorithm with absolute performance bound 2", *SIAM Journal on Computing*.

this case, the subset $\mathcal{F}_2 = B_{l*}$ could be easily (in polynomial time) packed into the system capacity (line 16). Otherwise, we move the item with the greatest profit and the highest traffic class k, i.e., the most flexible one from $\mathcal{F}_2$ to $\mathcal{F}_1$ until the space of $\mathcal{F}_1$ is greater than the half of the system capacity (lines 19-22). Then, if the total profit of $\mathcal{F}_2$ is greater than the half of the optimal one (line 23), the algorithm ends and we keep $\mathcal{F}_2$ as the optimal set. Otherwise, we choose the set providing the largest total profit after comparing $\mathcal{F}_2$, without the latest added element, with $\mathcal{F}_1$.

The proposed algorithm provides a performance ratio of at most $\frac{5}{2} + \epsilon$. The first 5 rows of our algorithm are executed $O(n^2)$ times, corresponding to the number of knapsack problems $P(C_l)$ to be solved. Given that the knapsack problem solution can be solved with $O(n \log n)$ computational time, the complexity of the Network Slices Packer is dominated by $O(n^3 \log n)$.

Forecasting-aware Network Slicer. When the forecasted information is available, the admission control gets more room to fit more network slice requests, while still meeting the slice SLAs guarantees. The algorithm is inspired in the concept of simulated annealing [17]. The additional complexity is due to the feasibility check of admitting a given set of items into the system, as packing items in a different order might influence the solution optimality in the next attempts.

We adopt a coding scheme called *sequence pair* [18] to represent candidate solutions of Problem ADM-CONTROL. With this scheme, a solution is represented by a pair of permutations of $|\mathcal{I}|$ items $\{\pi_+, \pi_-\}$. The π_+ permutation indicates the spatial relation between items on the horizontal axis, i.e., if i is before j it should be allocated on the left of j. Similarly, π_- refers to the vertical axis. With this representation, the simulated annealing algorithm can easily change the permutations by checking at every step kk whether the new locations are (i) feasible and (ii) provide a greater objective function value, i.e., $\Delta F = F_{kk+1}(x) - F_{kk}(x) > 0$. Additionally, solutions with lower objectives are also accepted with a certain admission probability $Pr_a(\Delta F) = \frac{\Delta F}{Tr}$, where Tr is the temperature obtained by the logarithmic cooling function $Tr_k = \frac{Tr_0}{ln(1+kk)}$ and Tr_0 is the initial temperature.

The Forecasting-aware Network Slicer algorithm starts by sorting in non-increasing order the slice requests according to their profits (c_i) and traffic class (k). At each step kk, the algorithm decides to shuffle permutations π_+, π_-, add a new item into both sets or remove an existing one. The algorithms stops when the temperature Tr has reached a zero value and no better solutions are found in the successive steps. While this algorithm asymptotically finds the global optimal solution, the running time might not be affordable. In Section VII, we propose some techniques to improve the computational efficiency and analyze the resulting complexity.

VI. Scheduling network slice traffic

Once the decision of which network slices to admit has been taken, we need to properly schedule the traffic of those slices. To this end, in the following we present a novel network slice scheduler that pursues the following two goals: (i) serving the tenant traffic of the granted network slices, and (ii) providing the required feedback to the forecasting process, yielding a closed-loop solution that drives the system to optimal performance (see Fig. 1).

A. Multi-class slice scheduler

We start by designing a scheduling algorithm that accounts for the different slice SLAs. We denote a traffic request from tenant i for traffic class k by $r_{i,z}^{(k)}$. We consider 6 traffic classes as described in Table I. Each traffic class is characterized by a time window $T^{(k)}$ identifying the time duration within which a class should see the rate it has been guaranteed $[z; z+1]$, which is shorter for high-demanding traffic requirements and larger for best-effort class. The scheduler ensures that the amount of committed resources is served within the given time window.

The key objective of our novel network slice traffic scheduler is to minimize consumed resources while guaranteeing the traffic SLAs within a network slice. When forecasted information is available, the scheduler expects slice traffic levels below the predicted traffic bounds i.e., $r_{i,z}^{(k)} \leq \hat{R}_{i,z}^{(k)}, \forall z \in L_i$. If forecasted traffic bounds are underestimated and the traffic demands exceed the expected values, the allocated resources may grow to a value as large as the value agreed during the slice request admission, i.e., $R_i^{(k)}$. In this case, slice allocations may overlap and traffic class requirements might not be satisfied incurring in slice SLA violations.

We formulate the scheduler problem as a general minimization problem addressing all traffic class SLAs. We let $s_{i,j}^{(k)}$ denote the scheduled traffic corresponding to the resource served at time j for each network slice, within the set of admitted slices $x_i^{(k)}$ available from the admission phase. The problem is formulated as follows

Problem SLICER-SCHEDULING:

$$\begin{aligned} \text{minimize} \quad & s_{i,j}^{(k)} \\ \text{subject to} \quad & \left(\sum_{j=zk+\bar{t}}^{zk+\bar{t}+T^{(k)}} s_{i,j}^{(k)} \right) \geq r_{i,z}^{(k)} x_i^{(k)}, \ \forall z \in \left[0, \left\lceil \frac{L_i}{T^{(k)}} \right\rceil - 1\right]; \\ & \sum_{i \in \mathcal{N}} s_{i,j}^{(k)} \leq \Theta + P_{i,j}^{(k)}, \quad \forall j \in \mathcal{L}; \\ & s_{i,j}^{(k)} \in \mathbb{R}_+, \qquad \forall i \in \mathcal{N}, j \in \mathcal{L}, k \in \mathcal{K}; \end{aligned}$$

where Θ is the total capacity of the system, given by the total amount of resource blocks, whereas $P_{i,j}^{(k)}$ is the penalty incurred for not having satisfied a particular tenant slice traffic SLA, i.e., a SLA violation. The network slice scheduler keeps track of SLA violations to promptly trigger dynamic forecasting parameters adjustments (as explained next).

B. Online Reinforcement Learning

As explained above, forecasting process failures may lead admission control to overbook available network resources, yielding SLA violations. A monitoring procedure is designed to keep track of the number of such violations and provide as feedback to the forecasting phase the penalty value $P_{i,j}^{(k)}$ in Problem SLICER-SCHEDULING. From Eq. (4), we can derive the forecasting error probability for a generic traffic class k as follows

$$\chi_i^{(k)} \, : \, h_i^{(k)} \Omega_\chi \sqrt{Var(e_{i,z}^{(k)})} = \hat{d}_i^{(k)} \tag{6}$$

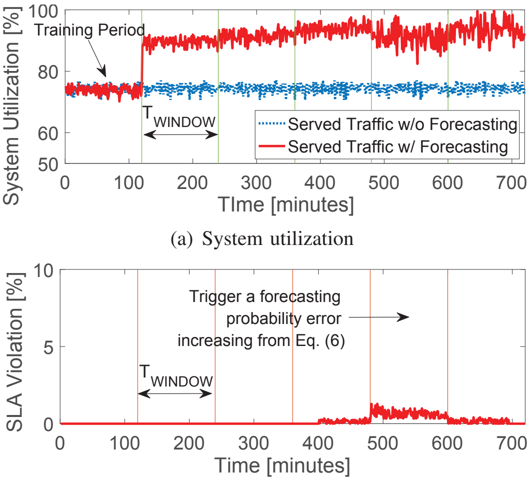

(a) System utilization

(b) SLA Violations

Fig. 5: System performance comparison with and without forecasting preprocessing.

where $h_i^{(k)}$ is the penalty history function, defined as $h_i^{(k)} = e^{\frac{nm}{W_S+nm}}$ assuming nm as the number of times the penalty is null and W_S as the length of the season considered in the forecasting process. The penalty history function drives the system from a setting where a higher forecasting error probability may be experienced to a more conservative setting, where no SLA violation occurs. Thus, in case of forecasting failures, a larger forecasting error probability is derived pushing the system towards a more conservative setting, with smaller gains.

VII. Performance Evaluation

We carried out an exhaustive simulation campaign to validate our framework. Our system is evaluated through an ad-hoc simulator developed in MATLAB®with a dual Intel(R) Xeon CPU 2.40GHz 4-cores and 16GB RAM. A summary of the simulation parameters used is provided in Table II. The system includes $|\mathcal{B}| = 7$ base stations ([19]) and $|\mathcal{I}| = 10$ tenants ([1]). The average number of users associated with a tenant is $E[|\mathcal{U}_i|] = 100$, which are distributed uniformly. When they move, a SLAW model is applied [14]. Tenant slice requests may range between the 5% and the 25% of the total system capacity, while their duration ranges between 1000 and 3600s. $P_{i,k}$ defines the probability that a slice request reaches the network within a time window. At the beginning of each T_{WINDOW} the admission control procedure is invoked. Based on the forecasting information, network slice requests are granted for the next time window and the associated slice traffic served.

A. Dynamics and SLA violations

A dynamic analysis of our system is provided here. Since no other work in the literature has proposed a solution for addressing network slice request accommodation, we benchmark our proposal against a legacy solution wherein no forecasted information is available during the admission control phase. The results are shown in Fig. 5(a) for a long simulation period of 720 minutes in terms of system utilization $Ul = \Theta - \sum_{i,k} s_{i,j}^{(k)}, \forall j \in T_{\text{WINDOW}}$, based on Problem SLICER-SCHEDULING. After a prior training period, the forecasting process provides useful information to the admission control block. Based on such information, network slice requests are properly reshaped and more traffic requests are efficiently accommodated into the network capacity. The gain after the second time window is about 20%. While no SLA violation occurs, the forecasting process moves from a conservative behaviour to a more aggressive by reducing the safe margin, i.e., the forecasting error probability from Eq. (6), which visibly brings more gain in terms of system utilization. However, due to the randomness of the traffic requests issued to the system, forecasted information might underestimate the real traffic level resulting in a SLA violation, as shown in Fig. 5(b). This promptly triggers the penalty history function $h_i^{(k)}$ which increases the forecasting error probability in the next time window, thereby keeping the SLA violation under control. Interestingly, our solution boosts the system utilization up to 100% while incurring a small SLA violation per tenant request (about 1.8% in a very short period).

TABLE II: System parameters ([19])

Parameters	Values	Parameters	Values
$\lvert\mathcal{I}\rvert$	10	$\lvert\mathcal{B}\rvert$	7 (21 sectors)
$\lvert\mathcal{K}\rvert$	6	$E[\lvert\mathcal{U}_i\rvert]$	100
Θ	200 RBs	ISD	250m
T_{OBS}	3600 s	η	0
T_{WINDOW}	7200 s	$P_{i,k}$	$\frac{1}{\lvert\mathcal{I}\rvert\lvert\mathcal{K}\rvert}$
L_i	$\{1000; 3600\}$ s	R_i	$\{\Theta * 0.05; \Theta * 0.25\}$
α_{SLAW}	3	Av. Speed	1.5m/s
ρ_{SLAW}	2.5	α_{DISTR}	1.5

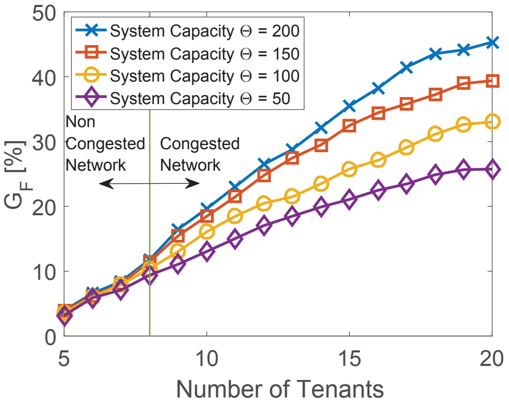

Fig. 6: System utilization gain for different network scenarios.

B. System Capacity Utilization

The effectiveness of the forecasted information is evaluated through a number of network scenarios. In Fig. 6, we consider 4 scenarios where the infrastructure provider decides to lease different portions of its own available resources, (i.e., Θ) from 50 to 200. The results are obtained for the forecasting case and the legacy option, after averaging them over 12 hours time period. We plot the relative gain $G_F = \left(\frac{\bar{Ul}_F}{\bar{Ul}_L} - 1\right)\%$, where $\bar{Ul}_F$ and $\bar{Ul}_L$ are the average utilization value of the forecasting and legacy solution, respectively.

We observe that the relative gain increases (i) with the number of tenants, and (ii) with the system capacity. Indeed, a small number of tenants implies a few network slice requests which can easily be fully accommodated, leading to a small relative gain. As soon as the network becomes congested, i.e., some network slice requests must be rejected, the utilization

TABLE III: Empirical complexity analysis

No. of tenants	10		20		30	
No. of slice req.	30 - 60		60 - 120		90 - 180	
Algorithms	**slices [no.]**	**time [sec]**	**slices [no.]**	**time [sec]**	**slices [no.]**	**time [sec]**
Network Slices Packer	9.584	78.1	11.337	215.7	13.226	497
Forecasting-aw. Network Slicer	9.607	129.5	**13.061** (11.897)	**714** (600)	**15.81** (13.307)	**3514.4** (600)

of our proposal outperforms the legacy scheme ($G_F \gg 0$) due to a wider distribution of network slice request values. On another angle, when the system capacity increases, there is more room to accommodate the network slices into the system, which leads to better performance. This provides an incentive to the infrastructure provider to lease much network resources as possible, to improve the overall system utilization.

C. Algorithm Complexity

We finally provide an empirically study of the computational cost for the two admission control algorithms proposed. For a fair comparison, we apply the algorithm to the same instances of the problem and average the results over several instances (100). We only compare the case where regular network slice shapes are considered.

In Table III, we show the results for different number of tenants present in the system. The results are expressed in terms of number of slices admitted into the system capacity and time elapsed for getting a response to an admission request. The average number of network slice requests within a single instance of the problem ranges from 30 (with 10 tenants) to 90 (with 30 tenants). Interestingly, the Forecasting-aware Network Slicer algorithm outperforms the Network Slices Packer, but it also experiences a longer computational time. We apply a time limit $T_Z = 600$s to avoid the process starvation. Given the long-term execution (every 30 minutes) of those admission control algorithms, this time bound is still acceptable for the overall system implementation. Nonetheless, the Forecasting-aware Network Slicer algorithm shows reasonable results in an affordable computing time.

Conversely, when irregular shape patterns are considered, the time complexity of the Forecasting-aware Network slicer further increases. This may become a significant drawback when the number of network slice requests is greater then 50. We overcome this problem in the following way. We first apply the network slices packer algorithm for the case with regular shapes. This provides an initial state for the Forecasting-aware Network slicer, which then starts exploring the neighbouring solutions to check whether they fit into the system capacity. In this way, we are able to reduce the computational time of the Forecasting-aware Network slicer by 20%, making it suitable for realistic deployments.

VIII. Conclusions

In this paper we have presented a comprehensive solution that involves network slicing traffic forecasting, admission control and scheduling for a 5G Network Slice Brokering system. The forecasting solution designed builds on Holt-Winters theory to predict future traffic levels per network slice, considering different service classes, and is effective in maximizing the number of requests that can be admitted by the an admission control decision engine. The admission control solution has been mapped into a geometric knapsack problem and two low-complexity algorithms have been designed for regular and irregular network slice requests, respectively. The network slice scheduling solution keeps track of SLA violations per slice and feeds this back to the forecasting engine such that it can adaptively adjust its behavior. Our main findings can be summarized as follows: i) Holt-Winters theory can be effectively applied to network slicing traffic forecasting both for regular and irregular slice requests, ii) elastic traffic network slice requests help in increasing the maximum achievable system utilization, iii) the forecasting benefits increase as the number of network slice requests and system capacity increases, and iv) low SLA violation risk levels result in very significant system utilization gains.

References

[1] NGMN Alliance, “NGMN 5G White Paper,” Tech. Rep. Version 1, Feb. 2015.

[2] K. Samdanis, X. Costa-Perez, and V. Sciancalepore, “From Network Sharing to Multi-tenancy: The 5G Network Slice Broker,” *IEEE Communications Magazine*, vol. 54, no. 7, Jul. 2016.

[3] Third Generation Partnership Project (3GPP), “Study on Radio Access Network (RAN) Sharing enhancements,” 3GPP TS 22.852, Sep. 2014.

[4] H. Wen and P.K. Tiwary and T. Le-Ngoc, *Wireless Virtualization*. Springer International Publishing, 2013.

[5] Third Generation Partnership Project (3GPP), “Network Sharing; Architecture and Functional Description,” 3GPP TS 23.251, Jun. 2016.

[6] ——, “Telecommunication management; Network Sharing; Concepts and requirements,” 3GPP TS 32.130, Jun. 2016.

[7] R. Mahindra, M. A. Khojastepour, H. Zhang, and S. Rangarajan, “Radio access network sharing in cellular networks,” in *Proceedings of the 21st IEEE International Conference on Network Protocols (ICNP)*, Oct. 2013, pp. 1–10.

[8] R. Kokku, R. Mahindra, H. Zhang, and S. Rangarajan, “NVS: A substrate for virtualizing wireless resources in cellular networks,” *IEEE/ACM Transactions on Networking*, vol. 20, no. 5, pp. 1333–1346, Oct. 2012.

[9] X. Costa-Perez, J. Swetina, T. Guo, R. Mahindra, and S. Rangarajan, “Radio access network virtualization for future mobile carrier networks,” *IEEE Communications Magazine*, vol. 51, no. 7, pp. 27–35, Jul. 2013.

[10] J. S. Panchal, R. D. Yates, and M. M. Buddhikot, “Mobile network resource sharing options: Performance comparisons,” *IEEE Transactions on Wireless Communications*, vol. 12, no. 9, pp. 4470–4482, Sep. 2013.

[11] G. Tseliou, K. Samdanis, F. Adelantado, X. Costa, and C. Verikoukis, “A capacity broker architecture and framework for multi-tenant support in LTE-A networks,” in *Proceedings of IEEE International Conference on Communications (ICC)*, May 2016.

[12] “Forecasting models and prediction intervals for the multiplicative holtwinters method,” *International Journal of Forecasting*, vol. 17, no. 2, pp. 269 – 286, Jun. 2001.

[13] Third Generation Partnership Project (3GPP), “Technical Specification Group Services and System Aspects; Policy and charging control architecture,” 3GPP TS 23.203, Jun. 2016.

[14] K. Lee, S. Hong, S. J. Kim, I. Rhee, and S. Chong, “SLAW: Self-similar least-action human walk,” *IEEE/ACM Transactions on Networking*, vol. 20, no. 2, pp. 515–529, Apr. 2012.

[15] K. Jansen and G. Zhang, “Maximizing the total profit of rectangles packed into a rectangle,” *Algorithmica*, pp. 323–342, Mar. 2007.

[16] H. Kellerer and U. Pferschy, “A new fully polynomial time approximation scheme for the knapsack problem,” *Journal of Combinatorial Optimization*, vol. 3, no. 1, pp. 59–71, Jul. 1999.

[17] A. Liu, J. Wang, G. Han, S. Wang, and J. Wen, “Improved simulated annealing algorithm solving for 0/1 knapsack problem,” in *Proceedings of the 6th International Conference on Intelligent Systems Design and Applications*, Oct. 2006, pp. 1159–1164.

[18] H. Murata, K. Fujiyoshi, S. Nakatake, and Y. Kajitani, “VLSI module placement based on rectangle-packing by the sequence-pair,” *IEEE Transactions on Computer-Aided Design of Integrated Circuits and Systems*, vol. 15, no. 12, pp. 1518–1524, Dec. 1996.

[19] ITU-R, “Guidelines for evaluation of radio interface technologies for IMT-Advanced,” Report ITU-R M.2135-1, Dec. 2009.